

Critical Slip Surface Search in Seismic Stability Assessment of Slope/Foundation

Kazumoto Haba¹, Kazuaki Watanabe²

¹ Manager, Taisei Corporation, Shinjuku, Tokyo, Japan (hb-kzm00@pub.taisei.co.jp)

² Chief Manager, Taisei Corporation, Shinjuku, Tokyo, Japan

INTRODUCTION

In the seismic stability assessment of the slope/foundation for nuclear power plants in Japan, the stress field of the ground is estimated via two-dimensional Finite Element Method (FEM) analysis, and sliding safety factors on assumed slip surfaces are calculated based on the stress. Such an assessment requires the determination of the critical slip surface, which has the minimum safety factor, in the target ground in advance. However, it is difficult to predict the critical slip surface, which is non-circular in complex geological models.

The optimization method can be used for determining the critical slip surface. Thus far, various search methods for critical slip surfaces using optimization methods have been proposed (Kim and Lee (1997), Goh (1999), Cheng et al (2007), Li et al(2010), Khajehzadeh et al (2012), Shinoda (2013), Bhandary (2019), Shinoda and Miyata (2019), Mishra et al (2019), Li et al (2020)). We have developed a particle swarm optimization (PSO) method to search for the critical slip surface based on a stress field obtained by FEM analysis (Shinohara et al. (2021), Haba et al. (2021)). The method enables the search for the noncircular critical slip surface appropriately and efficiently in geological models, including a failure surface, which is constructed with joint elements in FEM. In this study, the method was applied to a geological model, assuming a surrounding slope at nuclear power plant sites.

The remainder of this paper is organized as follows. First, the evaluation flow of the seismic stability assessment of the slope/foundation of nuclear power plants in Japan is reviewed. Next, the critical slip surface search method using PSO is presented. The method was then applied to a geological model. Finally, the conclusions are presented.

SEISMIC STABILITY ASSESSMENT OF SLOPE/FOUNDATION IN JAPAN

Figure 2 shows the evaluation flow of the seismic stability assessment of slopes/foundations for nuclear power plants in Japan, which is described based on the Japan Electric Association (2015). In the seismic stability assessment, an analytical model of the target ground is constructed based on a detailed geological survey. Some failure surfaces, such as fault planes, exist at nuclear power plant sites. failure surfaces are constructed using joint elements (Goodman (1976), Toki et al (1982)) in Finite Element Method (FEM). Next, the initial stress of the ground and the incremental seismic stress of the ground against standard seismic ground motion are estimated by static and dynamic FEM analyses, respectively. In this assessment, seismic analysis is conducted using equivalent linearization analysis. Subsequently, the sliding safety factor on the assumed slip surfaces is calculated based on the stress. Finally, the stability of the slope/foundation was assessed by comparing the safety factor and standard design criteria.

The sliding safety factor is defined as the ratio of the sum of the resisting force τ_R and the sum of the driving force τ_S along the assumed slip surfaces, as shown in Figure 2. The element average of stress is generally employed for calculating τ_R and τ_S using an equivalent linearization analysis. In this case, the safety factor is obtained using the following equation:

$$F_s = \frac{\sum_{m \in M} \tau_{Rm} \cdot l_m}{\sum_{m \in M} \tau_{Sm} \cdot l_m} \quad (1)$$

where m is the element ID and M is a set containing the ID of elements intercepted by a slip surface. τ_{Rm} and τ_{Sm} are the shear strength and shear force, respectively, along the segment of the slip surface in each element, and l_m is the length of the slip surface in each element. The shear strength is generally described by the Mohr-Coulomb theory in compression and becomes zero when tensile failure occurs.

$$\tau_{Rm} = \begin{cases} c_m + \sigma_{nm} \tan \phi_m & \text{(compressive)} \\ 0 & \text{(tensile)} \end{cases} \quad (2)$$

where c and ϕ are the cohesion and friction angles of the rock mass, respectively. σ_n is the normal stress on the slip surface.

The assumed slip surfaces are determined based on the position of the foundation base of important facilities, mobilized plane evaluated by static seismic intensity method analysis, and location of failure surfaces by engineers. The setting of the assumed slip surfaces requires many preliminary studies and engineering judgements. Furthermore, it is not necessarily that the assumed slip surfaces include the critical slip surface, which has the minimum safety factor. Therefore, a method for determining the critical slip surface based on the results of FEM analysis is required.

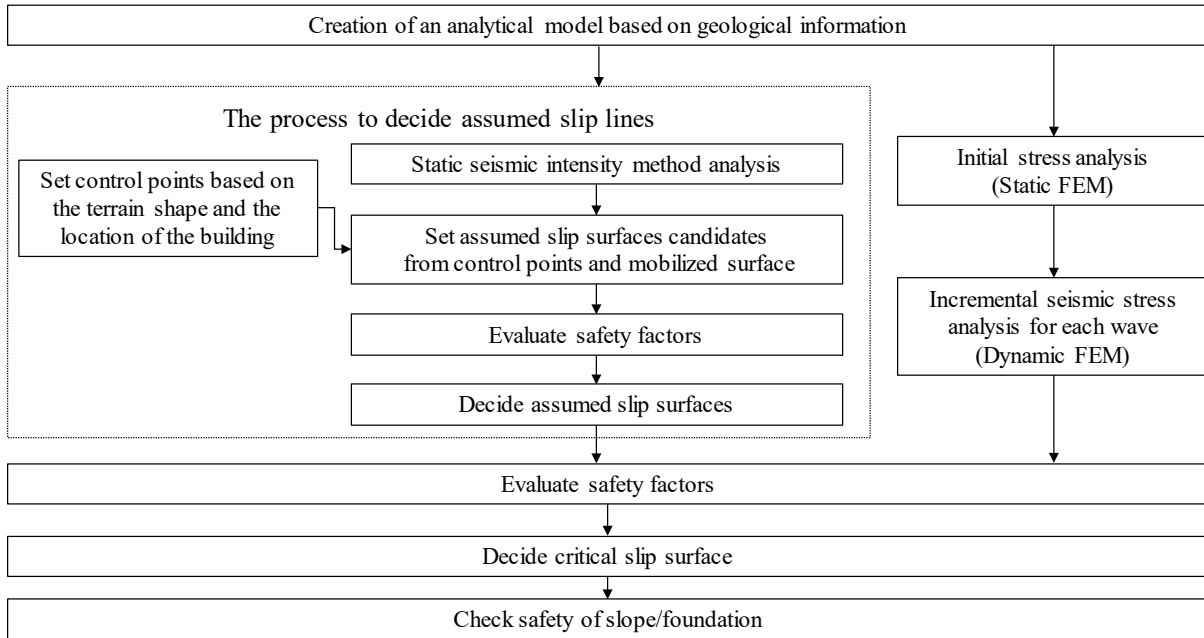


Figure 1. Seismic stability assessment of slope/foundation for nuclear power plants in Japan.

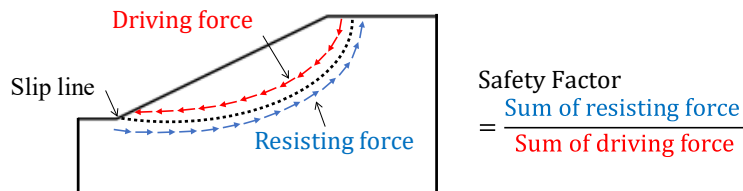


Figure 2. Conceptual diagram of sliding safety factor on a slip surface

METHOD FOR SEARCHING CRITICAL SLIP SURFACE

Particle Swarm Optimization

Particle Swarm Optimization (PSO) is an optimization method based on herd intelligence such as bird flocking (Kennedy and Eberhart (1995)). In this method, the particles move in the solution space while they exchange their information. Each position of particle P_i is updated using its velocity V_i : $P_i^{k+1} = P_i^k + V_i^{k+1}$. Herein, the indices of i and k are the particle ID and time step, respectively. The velocity of each particle is determined by considering its local best known position $P_{pb\ i}$ and the global best known position P_{gb} , as follows:

$$V_i^{k+1} = w \cdot V_i^k + c_{pb} \cdot r_{pb}^{k+1} \cdot (P_{pb\ i}^k - P_i^k) + c_{gb} \cdot r_{gb}^{k+1} \cdot (P_{gb}^k - P_i^k) \quad (3)$$

where w , c_{pb} , and c_{gb} are weight coefficients, and r_{pb} and r_{gb} are uniform random numbers in the interval $[0, 1]$. $P_{pb\ i}$ and P_{gb} are called the personal best and global best, respectively. Particles can eventually reach the optimum position even though they reach the local optimum position by exchanging the information of the global best P_{gb} .

PSO For Critical Slip Surface Search

When PSO is applied to the critical slip surface search, the particles and optimum solution correspond to the slip surfaces and critical slip surface, respectively. A slip surface is described as a polyline, and its position is defined as a set of positions of nodes of the polyline in our proposed method, as shown in Figure 4 A). The position of slip surface P_i is updated using the following equations:

$$P_i^{k+1} = P_i^k + V_i^{k+1} \quad (4)$$

$$V_i^{k+1} = w \cdot V_i^k + c_{pb} \cdot r_{pb}^{k+1} \cdot (P_{pb\ i}^k - P_i^k) + c_{gb} \cdot r_{gb}^{k+1} \cdot (P_{gb}^k - P_i^k), \quad (5)$$

where the personal best $P_{pb\ i}$ and global best P_{gb} are best known position of each slip surface and the best known position of all, respectively. r_{pb} and r_{gb} are diagonal matrices of uniform random numbers in the interval $[0, 1]$.

Figure 3 shows the evaluation flowchart of the proposed method. The method searches for the critical slip surface by repeating the calculation of the safety factor and updating the position of the slip surfaces. Furthermore, the critical slip surface can be efficiently searched for by gradually increasing the number of nodes in the polylines. The processing steps are as follows:

- Step A): The initial 40 slip surfaces are randomly generated for the target analytical model. Each initial slip surface is a circular slip surface approximated by a polyline with seven nodes.
- Step B): The safety factor of each slip surface is calculated using Equation 1 based on the results of the FEM analysis.
- Step C): Each personal best $P_{pb\ i}^k$ and global best P_{gb}^k are updated. Herein, $P_{pb\ i}^k$ and P_{gb}^k are obtained from the best positions of slip surface i and all surfaces until the current time step k , respectively.
- Step D): Convergence of a PSO process is confirmed using the change in safety factor δSF between time steps: $\delta SF < \epsilon_{\delta SF}$, and the velocity of each node $v_{i,n}$: $|v_{i,n}| < \epsilon_{i,n}$. Here, the tolerance $\epsilon_{\delta SF}$ was considered to be 0.001, which is determined considering significant digits for the safety factor in actual practices. Then, tolerance $\epsilon_{i,n}$ was determined based on the length of each line segment of the polylines.

- Step E): The positions and velocities of slip surfaces are updated using Equations 4 and 5. However, the velocities of the particles restrict the polyline from intersecting and exiting the model.
- Step F): Convergence of the search is confirmed using the change in safety factor ΔSF with an increasing number of nodes: ${}^{\alpha}\Delta SF < \epsilon_{\Delta SF}$. Here, $\epsilon_{\Delta SF}$ was considered to be 0.01, which is determined considering significant digits of the safety factor in actual practices and $\epsilon_{\delta SF}$. The search is completed when ${}^{\alpha}\Delta SF \leq \epsilon_{\Delta SF}$.
- Step G): Nodes are added at the center of all line segments when ${}^{\alpha}\Delta SF > \epsilon_{\Delta SF}$. As a result, the number of nodes increase from N to $2N-1$.

The slip surface, including a failure surface, can be searched using our proposed method. Because failure surfaces are constructed with joint elements with no thickness in FEM, it is difficult to search for the critical slip surface through joint elements using methods other than ours. The slip surface including the failure surface consists of a segment along the failure surface and two segments connecting the ground surface and the failure surface. Herein, the line segments between the ground surface and a failure surface are described by polylines, and part of the slip surface on the failure surface follows the shape of the failure surfaces, as shown in Figure 4 B). It should be noted that the line segment along the failure surface is not a polyline. The evaluation flowchart was the same as that shown in Figure 3.

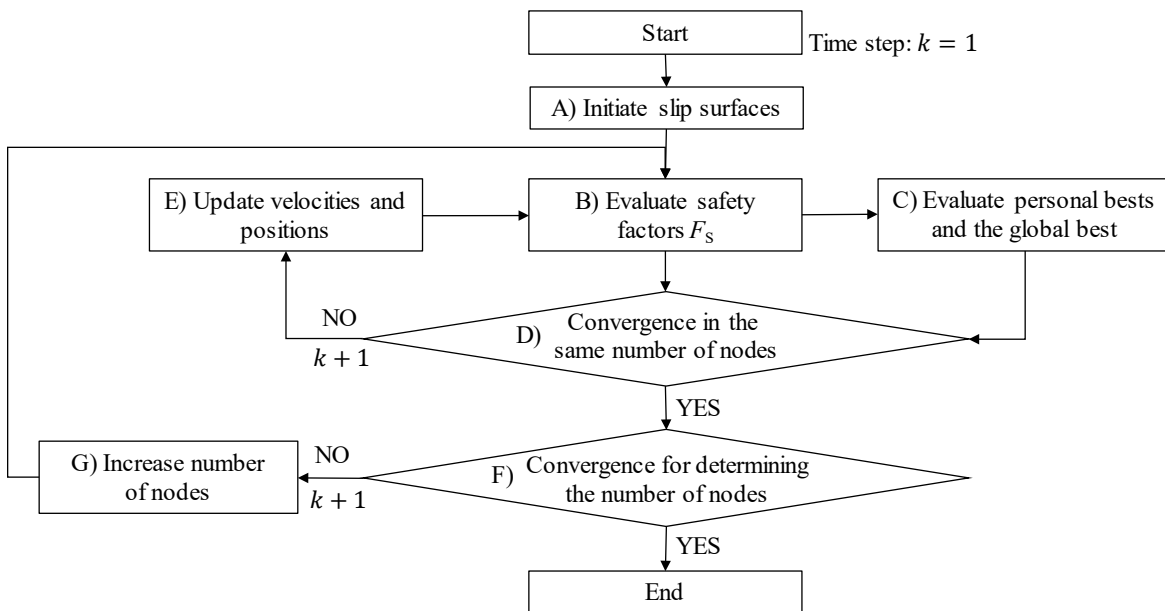
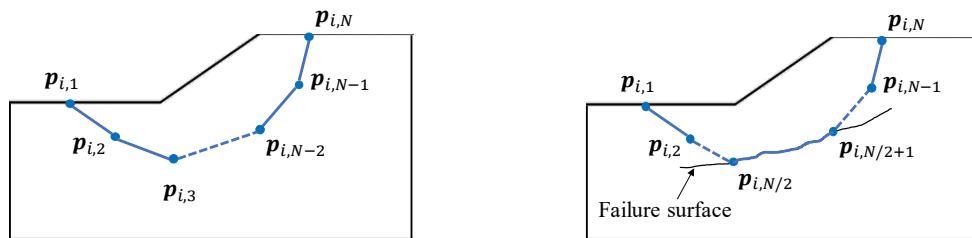


Figure 3. Evaluation flowchart for searching the critical slip surface using PSO.



A) passing through only rock mass B) passing through a failure surface
 Figure 4. Shape of a slip surface. $p_{i,n}$ denotes the position of node n in a slip surface P_i . N is the number of nodes.

RESULT AND DISCUSSION

In this section, we describe the result of search for the critical slip surface in a geological model, assuming a surrounding slope in nuclear power plant sites, by the proposed method. Figure 5 shows the analytical model. This model was created assuming a slope of soft rock, as shown in the technical documents of the Japan Society of Civil Engineers in 2009 (JSCE (2009)). However, the model was expanded in transverse and downward directions to suppress the influence of the boundary of the analytical model. Figure 6 shows the four assumed slip surfaces defined in technical documents. In this study, we statically loaded the self-weight and inertial force with leftward 0.15 G and downward 0.3 G. Moreover, tensile failure of rock mass was considered. Table 1 lists the material parameters of the soil, which were determined based on the dynamic characteristics of the soil. The area as shown by the red arrow in Figure 5 indicates a search area of the critical slip surface. In this study, we set the parameters of w , c_{pb} , and c_{gb} in Equation 5 to 0.8, which is the same as the previous studies (Shinoda (2013), Shinohara et al (2021) and Haba (2021)).

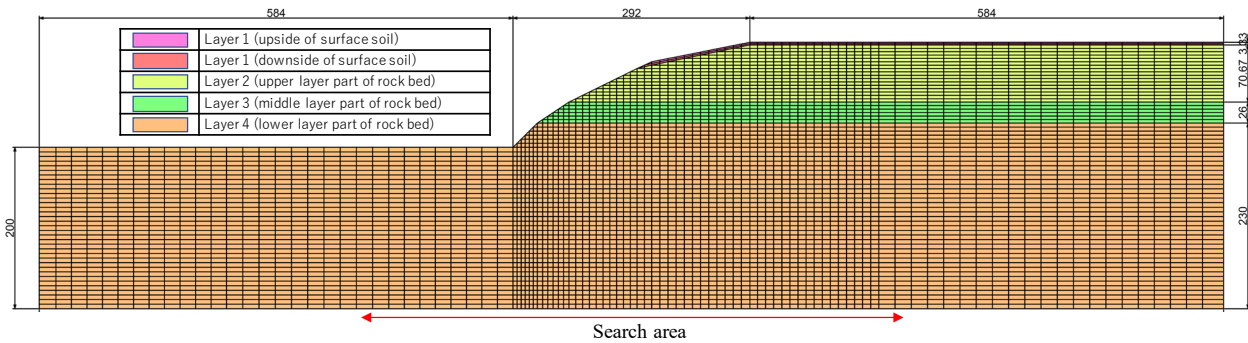


Figure 5. Analytical model created based on a geological model shown in the technical documents of JSCE (2009)

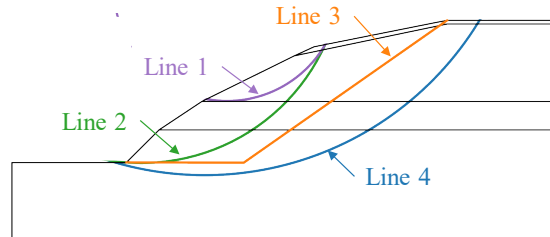


Figure 6. Assumed slip surfaces; these are defined in the technical documents of JSCE (2009).

Table 1: Material parameters of soil; these values are obtained from the dynamic characteristics shown in the technical documents of JSCE (2009).

Material Properties [unit]	Layer 1	Layer 2	Layer 3	Layer 4
Young's modulus [GPa]	0.47	0.98	1.3	2.0
Poisson's ratio [-]	0.45	0.43	0.43	0.42
Unit weight [kN/m ³]	18.0	17.0	18.0	19.0
Cohesion [kPa]	49+0.58 σ_0	1200	1400	1600
Friction angle [deg]	30	30	30	45

σ_0 : overburden pressure

Figure 7 shows the searched critical slip surface and its safety factor. Moreover, the figure shows the safety factor of the assumed slip surfaces. The searched critical slip surface has the smallest safety factor among all the surfaces and has a complex shape with a bend at the boundary of the geological layer. Therefore, it is difficult to set the complex critical slip surface without performing the analysis.

Figure 8 shows the relationship between the safety factor F_s and time step k . The number of nodes of the slip surfaces increases at the step indicated by the dashed lines. The number of nodes is 7 initially and increases to 13 and 25 at steps 55 and 106, respectively. The search is completed at step 151, in which the change in safety factor ΔSF with an increasing number of nodes becomes less than the tolerance of 0.01. Figure 9 shows the slip surfaces during the search. Only ten slip surfaces of the 40 ones are described in the figure. Herein, the search with $N = 7$ and 13 were converged at step 54 and 105, respectively. The slip surfaces, which are randomly located in the first step, move in the ground while reshaping and approaching the critical slip surface. Although the slip surfaces with $N = 7$ is similar to circular slip surface, the slip surfaces become more complex shapes having bends at the boundary of the geological layer by increasing the number of nodes in the polylines. The results indicate that the proposed method is highly effective for estimating the critical slip surface.

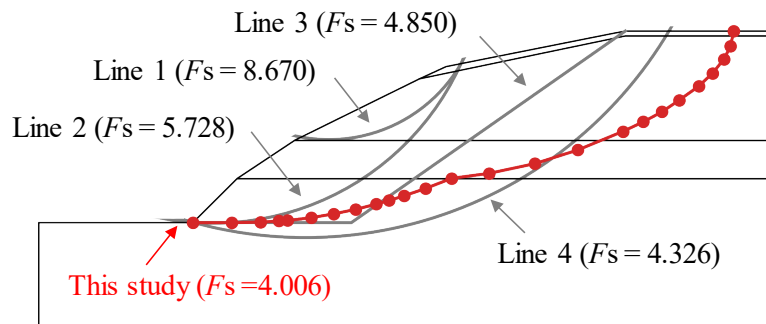


Figure 7. Critical slip surface and safety factor F_s estimated using the proposed method.

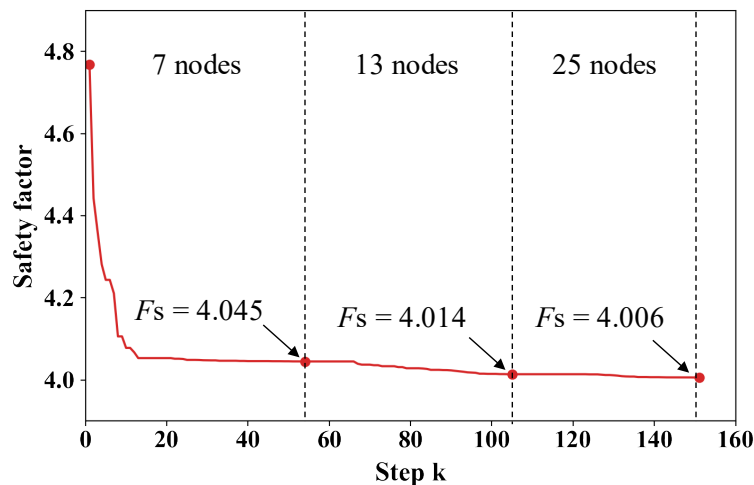


Figure 8. Relationship between safety factor F_s and time step k .

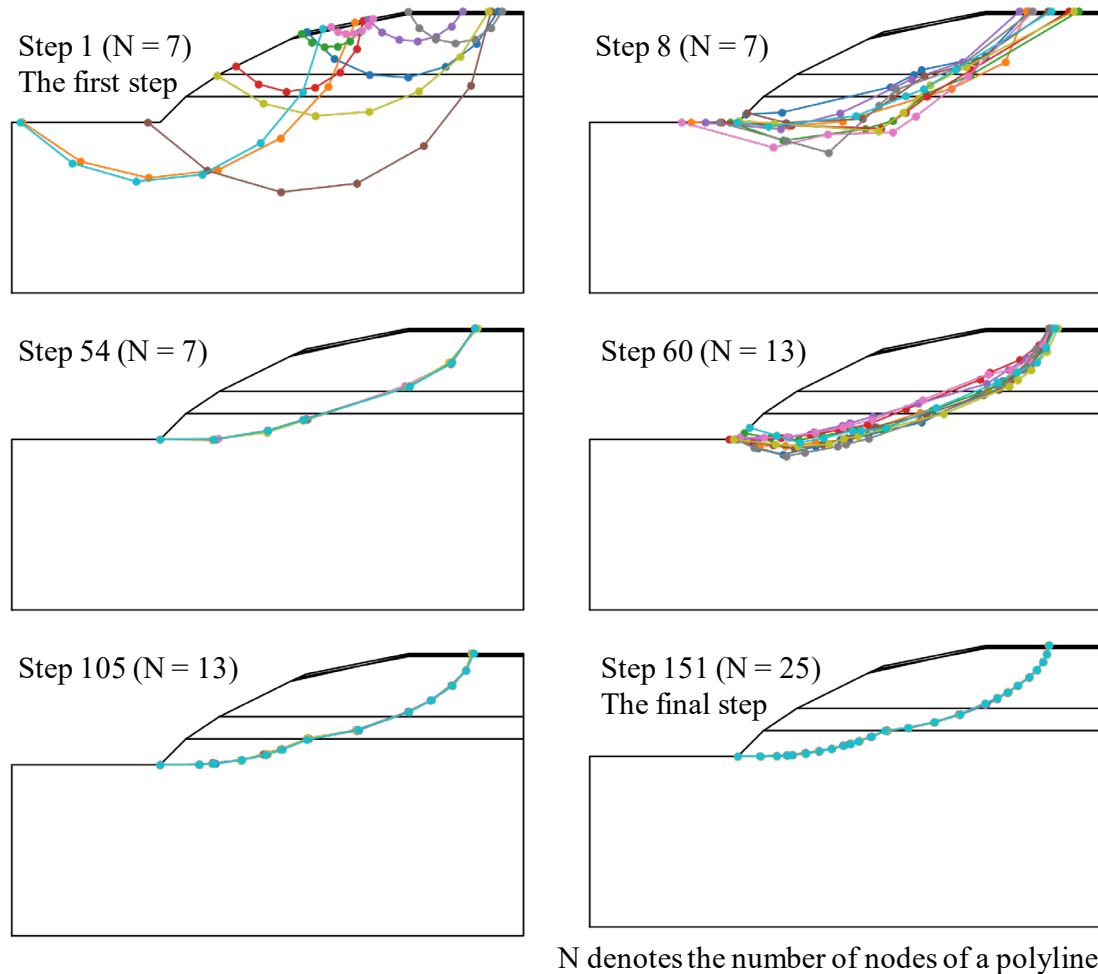


Figure 9. Slip surfaces during the search for critical slip surface

CONCLUSION

In the seismic stability assessment of foundation ground and surrounding slopes at nuclear power plant sites in Japan, the setting of the assumed slip surface requires many preliminary studies and engineering judgements. Therefore, the determining the critical slip surface in a complex ground model is difficult. We developed a method to search for the critical slip surface using PSO based on the stress of the ground evaluated by FEM analysis. This method can be used for searching the critical slip surface through a failure surface, such as a fault plane. In this study, we searched for the critical slip surface for a geological model assuming a surrounding slope at nuclear power plant sites and compared the results with the assumed slip surfaces. It was found that the method enables the critical slip surface to be searched appropriately and efficiently based on the results of FEM analysis in a complicated geological model.

REFERENCES

- Bhandary R. P., Krishnamoorthy, A. and Rao, A. U. (2019). "Stability Analysis of Slopes Using Finite Element Method and Genetic Algorithm," *Geotechnical and Geological Engineering*, 37, 1877-1889.
- Cheng, Y. M., Li, L. and Chi, S. C. (2007). "Performance Studies on Six Heuristic Global Optimization Methods in the Location of Critical Slip Surface," *Computer and Geotechnics*, 34 (6), 462-484.

- Goh, A. (1999). "Genetic Algorithm Search for Critical Slip Surface in Multiple-Wedge Stability Analysis," *Canadian Geotechnical Journal*, 36, 382-391.
- Goodman, R. E. (1976). "Methods of Geological Engineering in Discontinuous Rocks," *West Publishing Company*, Ch. 8, 300-368.
- Haba, K., Shinohara, K. and Watanabe, K. (2021). "A Search Method of Critical Slip Line with Quadratic Isoparametric Elements Using Particle Swarm Optimization," *Journal of JSCE A2*, 77(2), I_227-I_238. (in Japanese, with English abstract)
- Japan electric association, (2015). "Technical Guidelines for Aseismic Design of Nuclear Power Plants," *JEAG*, 4601-2015. (in Japanese)
- Japan Society of Civil Engineers. (2009). "Methodology for Evaluating the Stability of foundation Ground and surrounding slopes of Nuclear Power Plants [Technical documents]." (in Japanese)
- Kennedy, J. and Eberhart, R. (1995). "Particle Swarm Optimization," *Neural Networks, Proceedings, IEEE International Conference*, 4, 1942-1948,
- Khajehzadeh, M., Taha, M. R., El-Shafie, A. and Eslami, M. (2012). "Locating the General Failure Surface of Earth Slope Using Particle Swarm Optimization", *Civil Engineering and Environmental Systems*, 29, 41-57.
- Kim, J. Y. and Lee, S. R. (1997). "An Improved Search Strategy for the Critical Slip Surface Using Finite Element Stress Fields," *Computers and Geotechnics*, 21(4), 295-313.
- Li, S.H., Wu, L.Z., Luo, X.H. (2020). "A Novel Method for Locating the Critical Slip Surface of a Soil Slope," *Engineering Applications of Artificial Intelligence*, 94, 103733.
- Li, Y. C., Chen, Y. M., Zhan, T., Ling, D. S. and Cleall, P. (2010). "An Efficient Approach for Locating the Critical Slip Surface in Slope Stability Analyses Using a Real-Coded Genetic Algorithm," *Canadian Geotechnical Journal*, 47(7), pp. 806-820.
- Mishra, M., Gunturi, V.R. and Miranda, T.F.D. (2019). "Slope Stability Analysis Using Recent Metaheuristic Techniques: A Comprehensive Survey," *SN Applied Sciences*, 1, 1674.
- Shinoda, M. (2013). "Safety Factor Calculation of slopes by efficient search algorithm using noncircular slip surface," *Journal of JSCE C*, 69(4), 432-443. (in Japanese, with English abstract)
- Shinoda, M. and Miyata, Y. (2019). "PSO-Based Stability Analysis of Unreinforced and Reinforced Soil Slopes Using Non-Circular Slip Surface," *Acta Geotechnica*, 14, 907-919.
- Shinohara, K., Haba, K. and Watanabe, K. (2021). "Development of a Critical Slip Line Search Method for Stability Evaluation of Ground Using FEM," *Journal of Japan Association for Earthquake Engineering*, 21(5), 5_13-5_26. (in Japanese, with English abstract)
- Toki, K. Miura, F. and Otake, T. (1982). "Non-Linear Seismic Response Analysis of Soil-Structure Interaction System By 3-Dimensional Joint Element," *Proceedings of the Japan Society of Civil Engineers*, 322, 51-61. (in Japanese)